

Effects of graphite on ZnSb alloys as anode materials for lithium ion batteries^①

LÜ Chun-ping(吕春萍), ZHAO Xin-bing(赵新兵),
CAO Gao-shao(曹高劭), ZHU Tie-jun(朱铁军)

*Department of Materials Science and Engineering,
Zhejiang University, Hangzhou 310027, P. R. China*

Abstract: The electrochemical properties of multiphases $\text{Zn}_4\text{Sb}_3\text{C}_7$ and ZnSbC_2 as new lithium-ion anode materials were investigated. The composition and microstructures of these multiphase materials were analyzed by XRD and TEM. It was found that the addition of graphite modifies the microstructures of pure alloys. The capacities and the cycle stability of the anodes are greatly improved. The reversible capacity of $\text{Zn}_4\text{Sb}_3\text{C}_7$ reaches as high as 510 mAh/g at the first cycle, and keeps higher than 300 mAh/g after 10 charge/discharge cycles.

Key words: Zn_4Sb_3 ; ZnSb; multiphase anode material; lithium-ion battery

Document code: A

1 INTRODUCTION

Lithium-ion batteries are of the broadest interest in recent years because of their extraordinary merits such as high standard potential, high energy density, long cycle life and nonpollution.

The electrochemistry property of anode materials is one of the key factors that affect the energy density and performance of secondary lithium batteries. Graphite is now widely used for its layered structure which permits lithium-ion reversibly insert to and remove from the anode without significant volume change. But the theoretical capacity of graphite is only 372 mAh/g which is less than one tenth of metallic Li. Safety problem also exists for the low operating voltage of graphite against pure lithium. Although many kinds of pyrolyzed carbon with high capacity have been developed^[1~4], the drawback such as large irreversible capacity during the first cycle should not be overlooked.

Metals and alloys have been studied as anode materials since 1970^[5~8]. They have much larger capacity for Li than that graphite has. For example, metallic Sb can electrochemically alloy with Li up to about 4 Li per Sb which yields a maximum theoretical capacity of 715 mAh/g. Furthermore, the operating voltage may be chosen well above the potential of metallic Li, with which the problem of Li deposition during charging can be minimized and the safety of the batteries can be improved. One major problem to use metals and alloys as anode materials is the poor reversibility associated with the insertion and removal of Li^+ , since during these processes huge volume changes^[9] of the anode material and so that "crack-

ing" or "crumbling" of the anode may occur, from which the poor cycle life of the batteries results.

According to Besenhard^[10], some composites consisting of one reactive phase and one ductile phase could be the best anode materials for lithium-ion batteries. In view of these, multiphase $\text{Zn}_4\text{Sb}_3\text{C}_7$, ZnSbC_2 prepared by mechanical alloying of ZnSb alloys (ZnSb , Zn_4Sb_3 which is formerly studied as a potential thermoelectric material^[11,12]) with graphite are chosen as materials for lithium-ion anode in the present work. The composition, microstructure and electrochemical properties are investigated and the comparison between multiphase materials and pure alloys as anode materials are given.

2 EXPERIMENTAL

Commercial pure Zn and Sb with the mole ratio 4:3 were put into a quartz tube with the size of 14 mm × 100 mm. The tube was put into a furnace after it was pumped to 10^{-5} Pa and sealed. $\beta\text{-Zn}_4\text{Sb}_3$ was obtained by smelting the constituents at 750 °C followed by quenching.

The vacuum electric arc furnace for smelting (WS-2) was used to obtain the alloy of ZnSb. The starting materials were equimolar amounts of commercial pure Zn and Sb. The obtained alloys of Zn_4Sb_3 and ZnSb were analyzed using XRD.

It is believed that the particle size of anode materials directly affects the cycling performance. The smaller the grain sizes are, the better the electrochemical properties should be^[10]. And mechanical alloying has been proven to be an efficient processing technique to prepare powders with small grain size.

① **Foundation item:** Project 59771032 supported by the National Natural Science Foundation of China and project 97033518 supported by RFDP of the Education Ministry of China **Received date:** Aug.30, 1999; **accepted date:** Nov.22, 1999

So this nonequilibrium method was used to prepare all the samples.

The ball-milling was carried out in a conventional planetary ball mill. Powder mixtures of pure graphite and Zn-Sb alloys obtained as above-mentioned with different stoichiometry (Zn_4Sb_3 , ZnSb , ZnSbC_2) were ball-milled with the protection of petroleum ether. The mass ratio of the steel ball to powders was 25:1. After ball-milled for 100 h without interruption, the powders were dried and sifted. All the resultant samples were analyzed using XRD and the $\text{Zn}_4\text{Sb}_3\text{C}_7$ powder was also analyzed by TEM.

The testing electrodes were prepared by coating slurries of 95 % alloy powders and 5 % polytetrafluoroethylene (PTFE) on a foam nickel substrate with the size of $d10.0 \text{ mm} \times 1.5 \text{ mm}$. After coating, electrodes were pressed between steel plates at 18 MPa for 1 min, and then dried at 110°C for 24 h. A lithium foil (purity 99.9 %) was used as against electrode, and polypropylene paper (Celgard 2300) as microporous separator. The organic electrolyte was prepared by dissolving 1 mol/L vacuum dried LiClO_4 in 1:1 volume ratio mixture of ethylene carbonate (EC) and diethyl carbonate (DEC). All cells were assembled in an N_2 -filled glove box.

The electrochemical properties of the electrode were investigated by DC5 at 30°C under a dry atmosphere. The electrodes were charged / discharged between 0.005 V and 2.5 V, with the constant current of 30 mA/h/g.

3 RESULTS AND DISCUSSION

Fig. 1 shows the X-ray diffraction patterns of unmilled Zn_4Sb_3 , milled Zn_4Sb_3 and $\text{Zn}_4\text{Sb}_3\text{C}_7$. One can be seen that Zn_4Sb_3 obtained by smelting is ideally in β phase with well-crystallized structure. The X-ray diffraction patterns of unmilled ZnSb , milled ZnSb and ZnSbC_2 are shown in Fig. 2, from which it can be found that some Zn_4Sb_3 also exists in the ZnSb sample. Also in the $\text{Zn}_4\text{Sb}_3\text{C}_7$ and ZnSbC_2 sample, multiphase structures are obtained via ball-milling with the addition of graphite.

From Fig. 1 and Fig. 2. It can be seen that the increase in the width and the decrease in intensity of Bragg peaks of Zn_4Sb_3 after ball-milling are much more obvious than those of ZnSb . A possible interpretation for this has been suggested to be that during ball-milling process the complicated reaction between ZnSb and Zn_4Sb_3 in the ZnSb sample inhibits the decrease of crystallites. The addition of graphite to alloys accelerates effectively the process of decreasing the powder sizes so that the phenomena of the increase of the width and the decrease of the intensity of Bragg peaks of Zn_4Sb_3 are more obvious, especially for ZnSbC_2 . But the intensity of some peaks keeps high, which results from the superimposition with

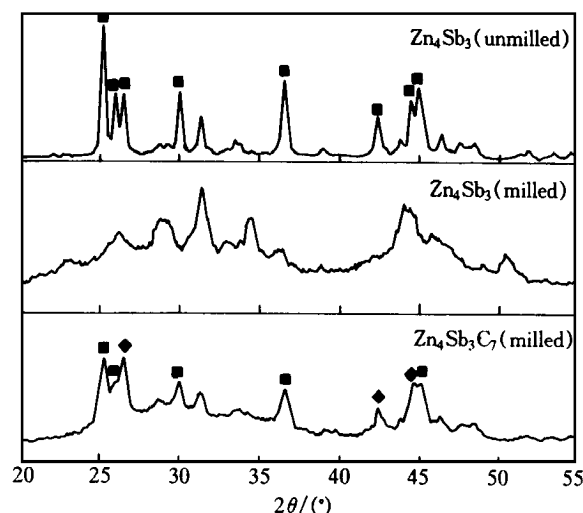


Fig. 1 X-ray diffraction patterns for unmilled Zn_4Sb_3 , milled Zn_4Sb_3 and $\text{Zn}_4\text{Sb}_3\text{C}_7$
■ — Zn_4Sb_3 ; ◆ — Peak of superimposition

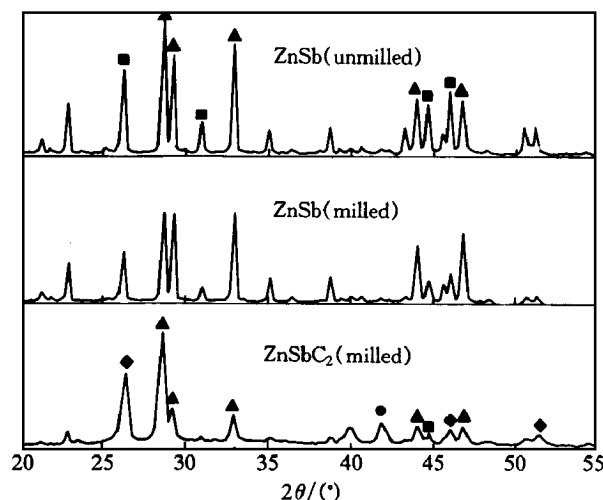


Fig. 2 X-ray diffraction patterns for unmilled ZnSb , milled ZnSb and ZnSbC_2

▲ — ZnSb ; ■ — Zn_4Sb_3 ; ● — C; ◆ — Peak of superimposition

peaks of both alloys and graphite.

Furthermore, the peak deviation of materials with ball-milling process is observed. For pure alloys, the occurrence of non-crystallization during ball-milling process is the reason. But for the multiphase materials of $\text{Zn}_4\text{Sb}_3\text{C}_7$ and ZnSbC_2 , small changes in crystal lattice resulting from the reaction of graphite and alloys could be another reason.

The TEM micrograph for $\text{Zn}_4\text{Sb}_3\text{C}_7$ is shown in Fig. 3, from which the black agglomeration alloys and the gray layered graphite can be seen. It is confident that multiphase material has been obtained with graphite distributing around alloys, although the distribution is some irregular.

Fig. 4 shows the first discharge (insertion of Li^+) and charge (desertion of Li^+) curves of Zn_4Sb_3

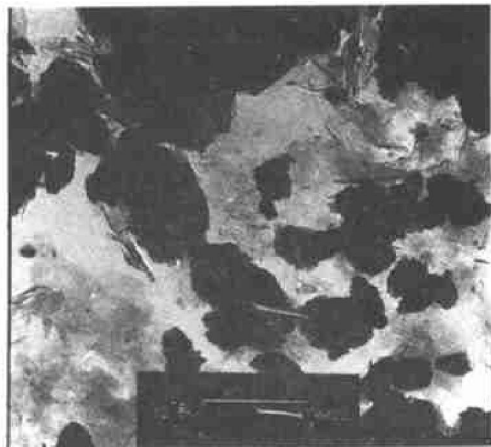


Fig.3 TEM micrograph for $\text{Zn}_4\text{Sb}_3\text{C}_7$

and $\text{Zn}_4\text{Sb}_3\text{C}_7$. The reversibility and reversible capacity are 58 %, 395 mAh/g for Zn_4Sb_3 and 59 %, 510 mAh/g for multiphase material of $\text{Zn}_4\text{Sb}_3\text{C}_7$, respectively. It is illustrated that with the addition of graphite, both the reversible and irreversible capacity can be improved.

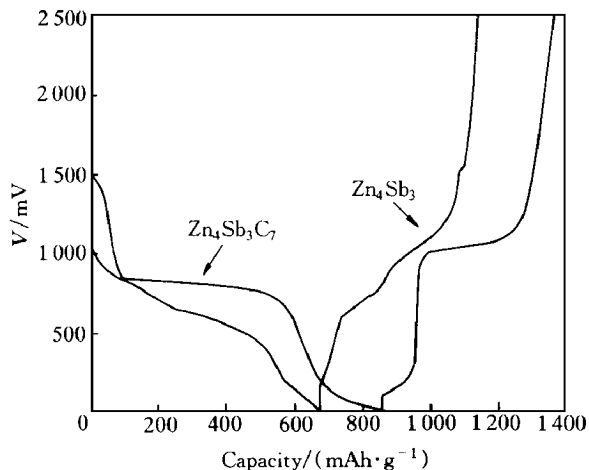


Fig.4 Voltage profiles for first cycle of cells with Zn_4Sb_3 and $\text{Zn}_4\text{Sb}_3\text{C}_7$

The capacity of the first discharge (Li^+ insertion) of Zn_4Sb_3 is 680 mAh/g. It means that $\text{Li}_{16}\text{Zn}_4\text{Sb}_3$ has formed which corresponds to Li-rich intermetallic phase Li_4Sb and LiZn ^[9]. It can be then considered that the theoretical maximum capacity is obtained. While for multiphase material of $\text{Zn}_4\text{Sb}_3\text{C}_7$, the capacity of the first discharge (Li^+ insertion) is 858 mAh/g which overruns its theoretical maximum capacity. The explanation for this phenomenon is probably due to Li^+ insertion into vacancies, microcravities and voids formed during ball-milling process with the addition of graphite.

In order to reveal the features of the potential

plateaus better, differential capacity vs voltage for the first cycle of the cells with Zn_4Sb_3 and $\text{Zn}_4\text{Sb}_3\text{C}_7$ are shown in Fig.5. From Fig.4, it can be seen that the potential plateau of multiphase material of $\text{Zn}_4\text{Sb}_3\text{C}_7$ is longer than that of Zn_4Sb_3 . Correspondingly the potential peak of $\text{Zn}_4\text{Sb}_3\text{C}_7$ is sharper than that of Zn_4Sb_3 . From the great difference between the dQ/dV curve of Zn_4Sb_3 and that of $\text{Zn}_4\text{Sb}_3\text{C}_7$, it can be concluded that the addition of graphite has greatly influenced the charge/discharge mechanism of anode material.

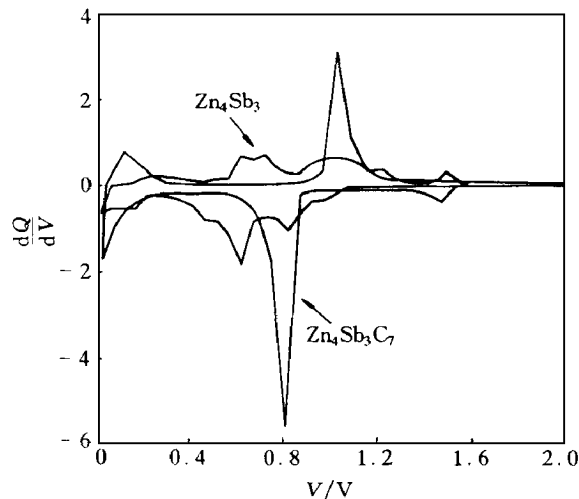


Fig.5 Differential capacity vs voltage for first cycle of cells with Zn_4Sb_3 and $\text{Zn}_4\text{Sb}_3\text{C}_7$

Furthermore, the multiphase material of $\text{Zn}_4\text{Sb}_3\text{C}_7$ has higher capacity than that pure alloy has for each charge/discharge process, as can be observed in Fig.6. The reason for this can be explained by the coexistence of small-sized Zn_4Sb_3 and very ductile graphite in $\text{Zn}_4\text{Sb}_3\text{C}_7$, an ideal kind of multiphase material suggested by Besenhard^[10]. It is well known that Li^+ insertion into alloy to form Li-rich intermetallic phase such as Li_4Sb and LiZn can significantly increase its volume^[9], which results in pulverization of anode. The cracks and powdering increase the contact impedance in the electrode and reduce the amount of lithium ions both inserting to and deserting from the anode. Therefore, the crumbling of alloys would significantly decrease the capacity. However, when the size of alloys is small enough, the crumbling rate may become slower resulting in improved electrochemical property^[10]. Further, in the multiphase material of $\text{Zn}_4\text{Sb}_3\text{C}_7$, the small-sized Zn_4Sb_3 particles are separated and microencapsulated by soft and ductile graphite. At the start of lithium insertion, only Zn_4Sb_3 alloy is expanded and becomes brittle, whereas the partly lithiated graphite still remains relatively soft and ductile, which decreases the crumbling rate of $\text{Zn}_4\text{Sb}_3\text{C}_7$. The advantage of a small particle-size

multiphase material for lithium insertion has been demonstrated recently also for tin-based metallic materials^[10].

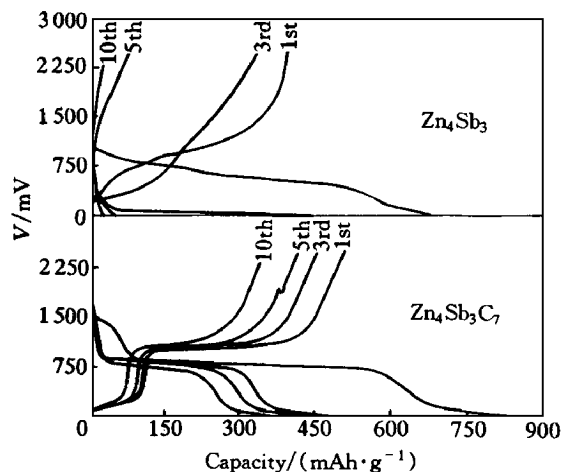


Fig. 6 Voltage profiles of 1st, 3rd, 5th, 10th cycle of cells with Zn_4Sb_3 and $\text{Zn}_4\text{Sb}_3\text{C}_7$

To further study the great effects of graphite on alloys as anode materials for lithium-ion batteries, we also chose ZnSb and ZnSbC_2 , another multiphase material, as the studied host. Fig. 7 shows their electrochemical properties. It can be found the similarity with Zn_4Sb_3 and $\text{Zn}_4\text{Sb}_3\text{C}_7$, namely the multiphase material of ZnSbC_2 has a higher capacity and longer cycling life than that of ZnSb .

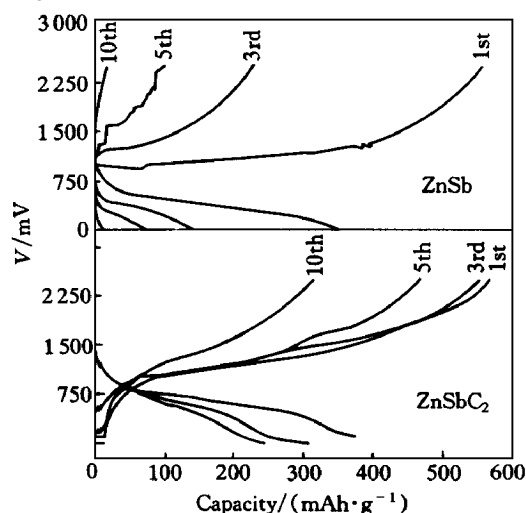


Fig. 7 Voltage profiles of 1st, 3rd, 5th, 10th cycle of cells with ZnSb and ZnSbC_2

The capacity as a function of cycle number of Zn_4Sb_3 and $\text{Zn}_4\text{Sb}_3\text{C}_7$ are compared in Fig. 8, while those of ZnSb and ZnSbC_2 are given in Fig. 9. The cycle lives of $\text{Zn}_4\text{Sb}_3\text{C}_7$ and ZnSbC_2 are much longer than those of Zn_4Sb_3 and ZnSb alloys, which indicates

that the cycle life also depends on the crumbling of pure alloys. Although anodes with pure Zn_4Sb_3 or ZnSb , have high capacities in the first cycle, the capacities decrease very fast and down to lower than 100 mAh/g after five cycles. While multiphase materials of $\text{Zn}_4\text{Sb}_3\text{C}_7$ and ZnSbC_2 have much improved cycle lives. Even after 10 charge/discharge cycles, the capacity keeps above 400 mAh/g, 300 mAh/g for $\text{Zn}_4\text{Sb}_3\text{C}_7$ and ZnSbC_2 , respectively. It is reconfirmed that in multiphase materials, the addition of graphite to pure alloys impedes the volume expansion of alloys resulting from Li^+ insertion and protect from the process of pulverization, so that leads to an improvement of both the capacities and cycle stability of the anode.

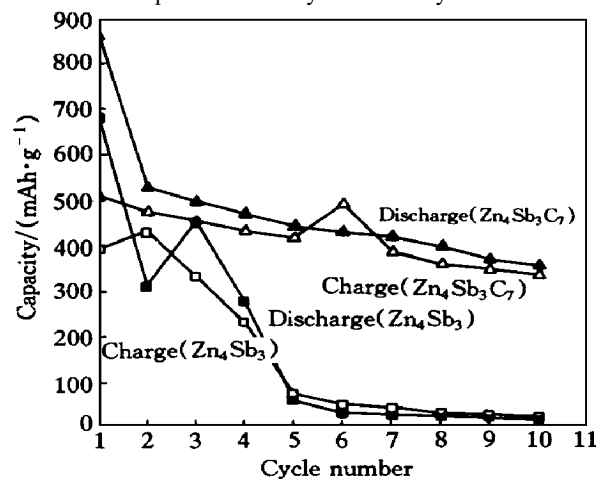


Fig. 8 Capacity as a function of cycle number for cells with Zn_4Sb_3 and $\text{Zn}_4\text{Sb}_3\text{C}_7$

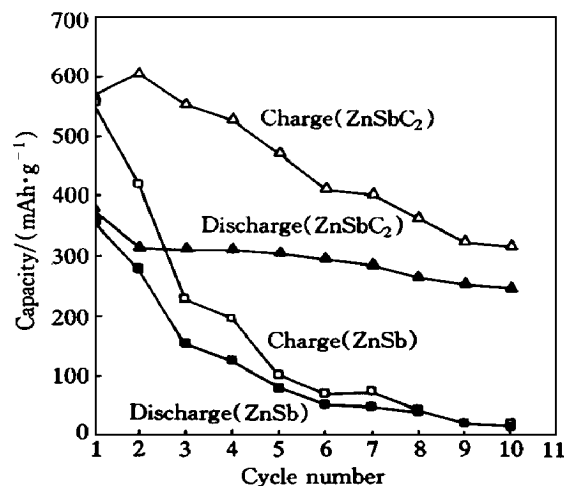


Fig. 9 Capacity as a function of cycle number for cells with ZnSb and ZnSbC_2

Also from Fig. 8, it can be found that occasionally, the Li -extraction capacity is more than the Li -insertion amount before, which maybe due to the unstable environment and irregular distribution of com-

ponents resulting from Li^+ insertion /extraction. While during the charge/discharge cycling process of ZnSb and ZnSbC_2 , the capacity of Li -extraction is always higher than the Li -insertion capacity, as can be observed in Fig.9. The reason for this anomaly phenomena is considered to be the complicated reaction between ZnSb and the impurity of Zn_4Sb_3 during cycling process. When analyzing the chemical composition of electrolyte, it is found that during the process of Li^+ extraction, not only Li^+ but also other element, e.g. Sb and Zn , are extracted from the anode.

4 CONCLUSIONS

Multiphase materials of $\text{Zn}_4\text{Sb}_3\text{C}_7$ and ZnSbC_2 are obtained by ball-milling method. With the addition of graphite, the cycling properties of the alloys are significantly improved. The first discharge capacity of $\text{Zn}_4\text{Sb}_3\text{C}_7$ is 858 mAh/g. Even after 10 charge/discharge cycles, the capacity keeps above 400 mAh/g, 300 mAh/g for $\text{Zn}_4\text{Sb}_3\text{C}_7$ and ZnSbC_2 , respectively. It is suggested that the addition of graphite to alloys inhibits the volume expansion of alloys resulting from Li^+ insertion and delays the process of pulverization. On the other hand, the addition of graphite has not increased the reversibility of the anode and eliminated the extraction of metallic elements from the anode.

REFERENCES

- [1] Tao Z, Yinghu L, Fuller E W, et al. Lithium insertion in high capacity carbonaceous materials [J]. *J Electrochem Soc*, 1995, 142(8): 2581 ~ 2590.
- [2] Xue J S and Dahn J R. Dramatic effect of oxidation on lithium insertion in carbons made from epoxy resins [J]. *J Electrochem Soc*, 1995, 142(11): 3668 ~ 3677.
- [3] Kenji Sato, Minoru Noguchi, Atsushi Demachi, et al. A mechanism of lithium storage in disordered carbons [J]. *Science*, 1994, 264(22): 556 ~ 558.
- [4] Norio T, Asako S, Takahosa O et al. Large hysteresis during lithium insertion and extraction from high-capacity disordered carbons [J]. *J Electrochem Soc*, 1998, 145(2): 478 ~ 482.
- [5] Mao Ou, Dunlap R A and Dahn J R. Mechanically alloyed Sn-Fe(-C) powders as anode materials for Li -ion batteries [J]. *J Electrochem Soc*, 1999, 146(2): 405 ~ 413.
- [6] Boukamp B A, Lesh G C and Huggins R A. All-solid lithium electrode with mixed-conductor matrix [J]. *J Electrochem Soc*, 1981, 128(4): 725 ~ 728.
- [7] Wang J, Raistrick I D and Huggins R A. Behavior of some binary lithium alloys as negative electrodes in organic solvent-based electrolytes [J]. *J Electrochem Soc*, 1986, 133(3): 457 ~ 460.
- [8] Chakravarti S K and Vetter J. A review on template synthesis: A membrane based technology for generation of nano-/micro-materials. *Solid State Phenomena*, 1997, 55(1): 80 ~ 85.
- [9] Fauteux D and Koksang R. Rechargeable lithium battery anodes: alternatives to metallic lithium [J]. *J Appl Electrochem*, 1993, 23(1): 1 ~ 10.
- [10] Yang J, Winter M and Besenhard J O. Small particle size multiphase Li -alloy anodes for lithium-ion batteries [J]. *Solid State Ionics*, 1996, 90(4): 281 ~ 287.
- [11] Tapiero M, Tarabichi S, Gies J G, et al. Preparation and characterization of Zn_4Sb_3 . *Electronic Materials*, 1985, 12(3): 257 ~ 274.
- [12] Kim Seong-Gon, Mazin I I and Singh D J. First-principles study of Zn-Sb thermoelectrics [J]. *Physical Review B*, 1998, 57(11): 6199 ~ 6203.

(Edited by HUANG Jin song)